ORIGINAL RESEARCH

Apolipoprotein E and Periostin Are Potential Biomarkers of Nasal Mucosal Inflammation

A Parallel Approach of *In Vitro* and *In Vivo* Secretomes

Youn Wook Chung[1,2,3*], Jimin Cha[3,4*], Seunghan Han[3,4], Yong Chen[5], Marjan Gucek[5], Hyung-Ju Cho[1,2,6], Kiichi Nakahira[7], Augustine M. K. Choi[7], Ji-Hwan Ryu[3,4‡], and Joo-Heon Yoon[1,2,6‡]

[1]The Airway Mucus Institute, [2]Global Research Laboratory for Allergic Airway Disease, [3]Severance Biomedical Science Institute, [4]Brain Korea 21 PLUS Project for Medical Science, and [6]Department of Otorhinolaryngology, Yonsei University College of Medicine, Seoul, Korea; [5]Proteomics Core Facility, National Heart, Lung and Blood Institute, National Institutes of Health, Bethesda, Maryland; and [7]Division of Pulmonary and Critical Care Medicine, Joan and Sanford I. Weill Department of Medicine, Weill Cornell Medicine, New York, New York

Abstract

No previously suggested biomarkers of nasal mucosal inflammation have been practically applied in clinical fields, and nasal epithelium–derived secreted proteins as biomarkers have not specifically been investigated. The goal of this study was to identify secreted proteins that dynamically change during the differentiation from basal cells to fully differentiated cells and examine whether nasal epithelium–derived proteins can be used as biomarkers of nasal mucosal inflammation, such as chronic rhinosinusitis. To achieve this goal, we analyzed two secretomes using the isobaric tag for relative and absolute quantification technique. From *in vitro* secretomes, we identified the proteins altered in apical secretions of primary human nasal epithelial cells according to the degree of differentiation; from *in vivo* secretomes, we identified the increased proteins in nasal lavage fluids obtained from patients 2 weeks after endoscopic sinus surgery for chronic sinusitis. We then used a parallel approach to identify specific biomarkers of nasal mucosal inflammation; first, we selected apolipoprotein E as a nasal epithelial cell–derived biomarker through screening proteins that were upregulated in both *in vitro* and *in vivo* secretomes, and verified highly secreted apolipoprotein E in nasal lavage fluids of the patients by Western blotting. Next, we selected periostin as an inflammatory mediator–inducible biomarker from *in vivo* secretomes, the secretion of which was not induced under *in vitro* culture conditions. We demonstrated that those two nasal epithelium–derived proteins are possible biomarkers of nasal mucosal inflammation.

Keywords: nasal epithelium; air–liquid interface culture; secretome; secreted proteins; mucosal secretions

Mucus hypersecretion is a common feature of several respiratory diseases, such as chronic rhinosinusitis (CRS), and is mainly caused by goblet cell hyperplasia, which is an epithelial abnormality (1). The upper airways are lined by a pseudostratified epithelium of ciliated, secretory, and basal cells (2). Basal cells were originally named based on their proximal location to the underlying basal lamina, and were recently found to include a population of multipotent stem cells that play important roles in both homeostasis of the normal epithelium and tissue regeneration after injury (3, 4).

Cells in the upper airway epithelium, such as nasal epithelial cells, are continuously exposed to environmental

(Received in original form August 3, 2018; accepted in final form June 12, 2019)

*These authors contributed equally to this work.

‡Co–senior authors.

This work was supported by grants from the Global Research Laboratory Program of the National Research Foundation of Korea (NRF) funded by the Ministry of Science, Information and Communications Technology (ICT), and Future Planning grant 2016K1A1A2910779 (J.-H.Y.), and from the Bio and Medical Technology Development Program of the NRF funded by the Ministry of Science, ICT, and Future Planning grant 2016M3A9D5A01952415 (J.-H.R.).

Author Contributions: Y.W.C., J.-H.R., and J.-H.Y. conceived and designed the study; Y.W.C., J.C., and H.-J.C. collected, processed, and analyzed samples; Y.W.C., S.H., Y.C., and M.G. conducted proteomics analysis; K.N. and A.M.K.C. analyzed the data; Y.W.C., J.-H.R., and J.-H.Y. analyzed the data and wrote the manuscript; all authors have reviewed and approved the final submission.

Correspondence and requests for reprints should be addressed to Joo-Heon Yoon, M.D., Ph.D., Department of Otorhinolaryngology, Yonsei University College of Medicine, 134 Shinchon-dong, Seodaemun-gu, Seoul 120-752, Korea. E-mail: jhyoon@yuhs.ac.

This article has a data supplement, which is accessible from this issue's table of contents at www.atsjournals.org.

Am J Respir Cell Mol Biol Vol 62, Iss 1, pp 23–34, Jan 2020

Originally Published in Press as DOI: 10.1165/rcmb.2018-0248OC on June 13, 2019
Internet address: www.atsjournals.org

stress including wall shear stress, temperature, humidity, and pathogens (5). Thus, proteins secreted from nasal epithelial cells during regeneration are essential to maintaining respiratory homeostasis (6, 7). Although inflammation is a crucial factor of wound healing and tissue regeneration, chronic inflammatory responses associated with CRS or asthma result in airway injury (8). Damage to the epithelium is an initial step in the process of airway remodeling, which is characterized by basal cell hyperplasia, goblet cell hyperplasia, and metaplasia (9). Accordingly, we predicted that nasal epithelium–derived proteins can be used as biomarkers to reflect the state of nasal mucosal inflammation, and can be detected in nasal lavage (NAL) fluid or nasal brushing, which is easily conducted in outpatient clinics.

Analysis of biological markers in NAL fluids provides valuable information for studying the nasal mucosal state, and enables monitoring of the results of medical and surgical treatments, because nasal secretions reflect the inflammatory state of the nasal mucosa. Various methods have been developed to obtain human nasal secretions, such as nasal irrigation, brush, scraping, and nasal secretion collectors, to analyze the biochemical components in nasal secretions (10). However, concentrations of biomarkers in nasal secretions vary, because the collection method directly influences the results obtained, limiting the applicability of these methods (11). Applicable biomarkers for studying inflammation in the nasal mucosa include eosinophil cationic protein, myeloperoxidase, tryptase, lysozyme, lactoferrin, and albumin (12–14). Many studies have sought to identify additional inflammatory biomarkers in nasal secretions; however, only IgE or IL-5 have been recently suggested as biomarkers specific to CRS with nasal polyps (15, 16). Epithelium-derived proteins have also been suggested as biomarkers, which were identified mostly by proteomics analyses of secretions from human primary airway epithelial cells, such as apolipoproteins (APOs), mucins, annexins, histones, bacterial/permeability-increasing proteins, S100 proteins, ceruloplasmin (CERU), lumican, and gelsolin (6, 17, 18).

Although APOs, the major structural component of lipoproteins, play critical roles in lipid uptake and transport, they were recently identified as potential biomarkers of inflammatory diseases, because of their involvement in cytokine and chemokine release, as well as cell adhesion molecule expression (19). In nasal mucus of patients with allergic rhinitis, APOA1 and APOA2 increase significantly (20) and are suggested to have anti-inflammatory functions in the colonic and pulmonary epithelium (21–23). In contrast, these proteins act as pro-inflammatory molecules because of posttranslational changes possibly mediated through oxidative mechanisms (24). Another APO, APOE, has been suggested as a biomarker of coronary artery disease or Alzheimer's disease (25). Periostin (POSTN), a secreted extracellular matrix protein, binds to integrin molecules to support adhesion and migration of epithelial cells, and is induced by IL-4 and IL-13 (26). Clinically, POSTN is involved in lung fibrosis and airway remodeling (27), inflammation and allergy (28), and progression of eosinophilic CRS with nasal polyps (29).

To identify and validate practical biomarkers for indicating the state of nasal mucosal inflammation, we first analyzed the human nasal secretome obtained from cultured primary HNECs according to the degree of differentiation, and then analyzed nasal secretions obtained from two groups of subjects. One group included patients who were scheduled to take septoplasty as a control group, because they had no inflammation in nasal mucosa. NAL fluids were collected just before septoplasty under general anesthesia in the operating room. The other included patients who underwent endoscopic sinus surgery for chronic sinus surgery as an experimental group. NAL fluids were collected at 2 weeks after surgery, which is the most active stage of nasal mucosal regeneration.

Methods

For additional information, detailed Methods are fully described in the data supplement.

Preparation of NAL Fluid Secretome from Patients

All participants provided informed consent, and this study was approved by the institutional review board of the Yonsei University College of Medicine (4-2016-0902 and 4-2016-1153). NAL fluids were collected from a control group (septoplasty patients, $n = 5$) just before septoplasty under general anesthesia or from an experimental group (chronic sinus surgery patients, $n = 13$) at 2 weeks after surgery. The mucosal status at 2 weeks after endoscopic sinus surgery (ESS) is typically an active regeneration stage, because complete mucosal regeneration after ESS requires approximately 3–4 months. All subjects had no allergic rhinitis as confirmed by the negative result of a skin prick test and serum allergen-specific IgE using multiple allergen simultaneous test (MAST). Patients with underlying immunologic diseases, such as malignancy, autoimmune diseases, or allergic asthma, were excluded (Table E1 in the data supplement). NAL fluid was collected as follows. Briefly, the patient was in the sitting position with the neck flexion on the chair at the outpatient clinic, and we instilled 10 ml normal saline into the middle meatus of the nasal cavity using a syringe with a cut-down needle to prevent injury to the nasal mucosa. Lavage fluid was recollected into a sterilized, 15-ml conical tube. All procedures were performed under endoscopic visualization to obtain lavage from the middle meatus. In postoperative patients, the lavage fluid was collected from the ethmoid sinus in the same manner at 2 weeks after surgery to detect secreted proteins during the wound healing process. For secretome preparation, cells and cell debris were removed by centrifugation at $18{,}506 \times g$ for 3 minutes. The resulting supernatants were mixed with six volumes of prechilled acetone and incubated overnight at -20°C. The secretome was precipitated by centrifugation at $8{,}000 \times g$ for 10 minutes at 4°C.

Isobaric Tag for Relative and Absolute Quantification

Isobaric tag for relative and absolute quantification (iTRAQ) proteomic methods with 8plex tags (SCIEX) were used to detect differences in protein expression in the NAL fluid from patients and mucus layer of human nasal epithelial cells (HNECs) during differentiation. All processes, including iTRAQ labeling, strong cation exchange fractionation, and liquid chromatography (LC)–mass spectrometry (MS), were performed as previously described (30), and database searching and quantitative data analysis were performed by Poochon Scientific.

Database search and quantitative data analysis. MS raw data files were searched against the human protein sequence

databases obtained from the National Center for Biotechnology Information website using Proteome Discoverer 1.4 software (Thermo) based on the SEQUEST and percolator algorithms, respectively. The false-positive discovery rate was set to 1%. The resulting Proteome Discoverer Report contains all assembled proteins with peptides sequences and peptide spectrum match counts (PSM#) and iTRAQ-tag–based quantification ratio. The iTRAQ-tag–based quantification was used to determine the relative abundance of proteins identified in the iTRAQ-ALI-4Ds (air–liquid interface [ALI]) data set. One-way ANOVA was used to identify proteins differentially secreted over time in ALI cultures, and was corrected using Bonferroni's multiple comparison test. The k-means clustering was performed and heat maps were generated using the heatmap.2 function of the R's gplots package (CRAN). Pearson's correlation coefficient was used to group based on the shape of expression profiles over time in ALI cultures. The volcano plots were drawn using R's ggplot2 package.

Results

Degree of Differentiation in Cultured Primary HNECs over Time

To investigate changes in the secretomes during epithelial cell differentiation, we used an *in vitro* primary cell culture system of HNECs. HNECs were freshly isolated from polyps and differentiated to a mucociliary epithelium with apical polarization according to the timetable depicted in Figure 1A. We determined the degree of differentiation by measuring the number of ciliated cells positive for Ac-α-tubulin, secretory cells positive for MUC5AC, basal cells positive for p63, and intermediate cells negative for all three antibodies by immunofluorescence microscopy (Figure 1B). At the initial stage of ALI culture Day 2 (ALI 2D), we observed that the cultures consisted largely of basal cells (38.10 ± 2.10%; Figure 1C), which expressed p63, a marker of basal cell differentiation (31). However, the number of basal cells was dramatically reduced by more than half during HNEC differentiation (18.15 ± 2.87% at ALI 15D; Figures 1C and Figure E1). In contrast, the number of MUC5AC-positive secretory cells gradually increased by 2.74%, 6.14%, and 15.57% at ALI 6D, ALI 10D, and

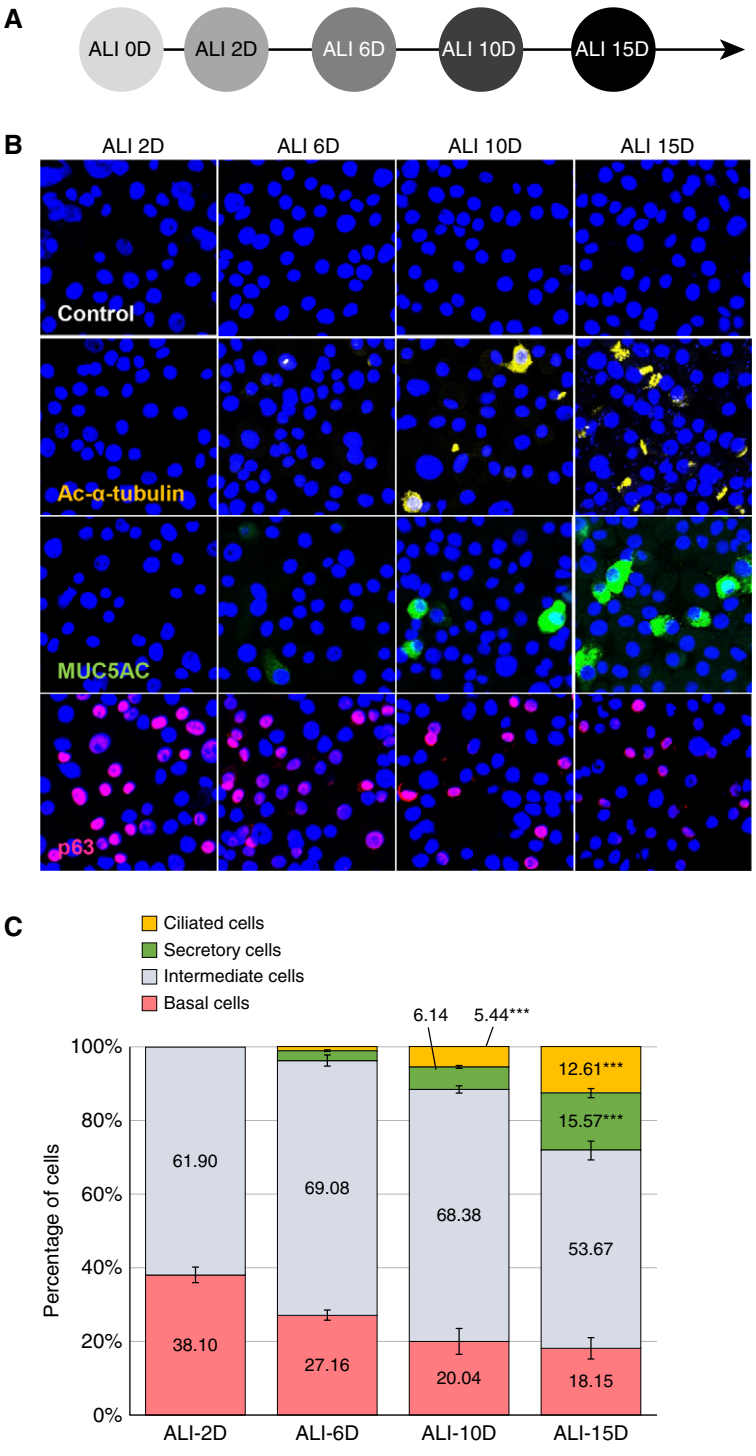

Figure 1. Changes in primary human nasal epithelial cell (HNEC) composition during differentiation. (*A*) Scheme of the HNEC differentiation during air–liquid interface (ALI) culture (e.g., ALI culture for 15 d [ALI 15D]). (*B*) HNECs in different stages of differentiation were analyzed by immunofluorescence staining of cytospin slides with antibodies against specific marker proteins; ciliated cells are shown as acetylated-α-tubulin (Ac-α-tubulin)–positive cells (yellow); secretory cells are shown as MUC5AC-positive cells (green); and basal cells are shown as p63-positive cells (red). (*C*) Percentages of ciliated, secretory, intermediate (subtracted the ciliated, secretory, and basal cell portions from total cell numbers), and basal cells during differentiation of HNECs are presented as bar graphs. Results are the means ± SEM; $n = 4$; ***$P < 0.001$ versus ALI 2D by one-way ANOVA with Bonferroni *post hoc* correction. MUC5AC = mucin 5AC, oligomeric mucus/gel-forming.

ALI 15D, respectively, and Ac-α-tubulin–positive ciliated cells reached a maximum (12.61 ± 1.25%) at ALI 15D, levels of which were nearly undetectable until ALI 6D (Figure 1C). We also estimated the number of intermediate cells, which was calculated by subtracting the number of ciliated cells, secretory cells, and basal cells from the total cell number (Figure 1C). Although the number of secretory and ciliated cells increased over time, the number of intermediate cells (~54–70% of cells) did not fluctuate until ALI 10D of HNEC differentiation (Figure 1C), indicating that differentiation from basal cells to intermediate cells occurred in our primary culture system.

Profiling of Mucins from HNECs

Mucosal layers were collected from the apical surface of HNECs at ALI 2D, ALI 6D, ALI 10D, and ALI 15D. For proteomic analysis, two sets of apical secretions were prepared and labeled with 8plex iTRAQ reagents (Figure 2A). Using the iTRAQ, we investigated the changes in the secretomes during HNEC differentiation. The iTRAQ (8plex) raw MS data files were analyzed with Proteome Discoverer 1.4 for protein identification and iTRAQ-based quantification. A total of 3,506 human proteins was quantitatively identified across four groups of eight samples in the iTRAQ-ALI-4Ds dataset (Figure 2A). Comparison of the protein profiles in terms of relative protein abundance between ALI 2D and ALI 6D (Figure 2B), ALI 2D and ALI 10D (Figure 2C), or ALI 2D and ALI 15D (Figure 2D) was performed. Most of the 215 housekeeping proteins were not changed in the eight samples after normalization, indicating that the dataset is reliable (Figures 2B–2D). A total of 269 proteins was significantly changed by at least twofold in three comparison groups ($P < 0.01$, $n = 2$)—37 proteins between ALI 2D and 6D (Figure 2B), 112 proteins between ALI 2D and 10D (Figure 2C), and 120 proteins between ALI 2D and 15D (Figure 2D)—demonstrating that the numbers of numerous proteins were altered when HNEC differentiated.

To verify our iTRAQ analysis results for the HNEC secretomes, we analyzed the raw MS data of mucins, the most abundant proteins in mucus. Mucins are high-molecular-weight glycoproteins synthesized by the submucosal glands and goblet cells of the human airway epithelium (32). MUC5AC and MUC5B belong to the gel-forming mucins, and MUC1, -4, -16, and -20 belong to the tethered mucins (32–34). Based on the total number of identified peptide sequences (Σ# PSMs) for the protein, the tethered mucin MUC16 was dominant (785 peptides); lower amounts of MUC1 (574 peptides) and MUC4 (322 peptides) were detected (Figure 2E and Table E2). Among the gel-forming mucins, MUC5B was the major mucin identified (273 peptides), with MUC5AC detected at a comparable level (66 peptides) (Figure 2F). However, MUC18 (9 peptides), MUC20 (9 peptides), and MUC21 (12 peptides) were present at a lower amount in the HNEC secretomes (Figure 2G). For further verification, we analyzed the temporal secretion profiles of mucins during HNEC differentiation. Secretions of the gel-forming mucins, MUC5AC and MUC5B, and tethered mucin, MUC16, increased progressively, whereas MUC1 and MUC4 were constitutively secreted with a slight increase at the initial stage of differentiation (Figures 2E and 2F). MUC18 was the only mucin, the secretion of which was significantly decreased. The other less-secreted mucins, MUC20 and MUC21, showed no changes in secretion (Figure 2G). Taken together, our results indicate that HNECs were well differentiated into either secretory cells or ciliated cells over time, and, as a result, gel-forming mucins increased, whereas most tethered mucins showed no changes or slight changes except for MUC16, the secretion of which was dramatically increased.

Pathway Analysis and Quantitative Proteomic Characterization of *In Vitro* HNEC Secretomes

To identify possible biological pathways involved in HNEC secretomes, we used the Database for Annotation, Visualization and Integrated Discovery (DAVID, version 6.8; Laboratory of Immunopathogenesis and Bioinformatics, National Institute of Allergy and Infectious Diseases, National Institutes of Health) tool. Kyoto Encyclopedia of Genes and Genomes (KEGG) pathway analysis demonstrated that 84 significant pathways ($P < 0.05$) were enriched in HNEC secretomes. Among them, the top 10 pathways were as follows: endocytosis (148 proteins); carbon metabolism (77 proteins); biosynthesis of antibiotics (118 proteins); proteasome (39 proteins); lysosome (72 proteins); bacterial invasion of epithelial cells (52 proteins); glycolysis/gluconeogenesis (45 proteins); protein processing in endoplasmic reticulum (86 proteins); biosynthesis of amino acids (45 proteins); and metabolic pathways (409 proteins). This finding was consistent with normal cellular development and functions (Figure 3A). Proteins were then classified by cellular compartment (CC) based on functional annotation with gene ontology (GO) analysis. Among the top 10 CC categories, 64.16% of GO items were associated with extracellular region, extracellular region part, extracellular organelle, extracellular vesicle, and extracellular exosome, indicating that, although there were some proteins from other CCs, such as membrane-bounded vesicles, cytosol, or junctions, a large number of HNEC secretomes were composed of secreted proteins (Figure 3B). To characterize the HNEC secretomes, we examined the most abundantly secreted proteins based on Σ# PSMs and listed the top 50 proteins in Table E2.

Quantitative Proteomic Profiling and Pathway Analysis of *In Vivo* NAL Fluid Secretomes

To gain more physiological and comprehensive insight into nasal mucosal secretomes, we analyzed human *in vivo* NAL fluid secretomes. By iTRAQ-based quantification, NAL fluid secretomes from the control group ($n = 5$) and the CRS group ($n = 4$) subjects who underwent ESS were examined. Because the NAL fluids were collected from patients with CRS 2 weeks after ESS, it was assumed that the mucosae of these patients were synchronized at a certain stage in regeneration. As such, we hypothesized that proteomic analysis of CRS NAL fluid secretomes would reflect a progression in regeneration, such as severe inflammation, and through comparison with HNEC secretomes, the degree of differentiation in the mucosae could be estimated.

A total of 660 human proteins were quantitatively identified in the 2 groups of 9 samples (five control vs. four patient samples) by database searching against a human protein sequence database obtained from the National Center for Biotechnology Information website using Proteome Discoverer 1.4 using 9 iTRAQ labeling tags (iTRAQ-H9 dataset) (Figure 4A). As shown in Figure 4B, 492 proteins overlapped: 74.55% of 660 *in vivo* secretomes and

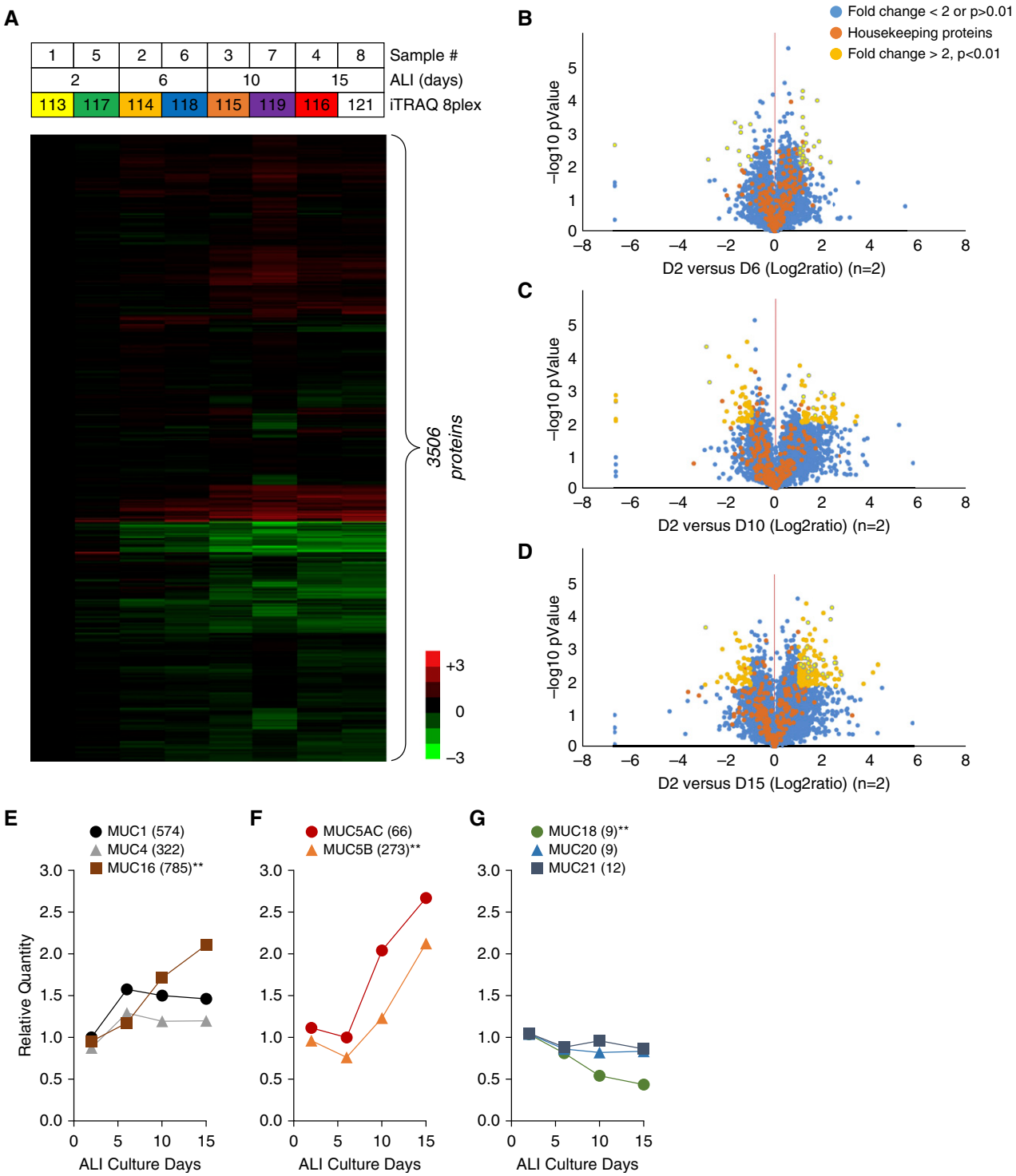

Figure 2. Proteomic characterization of secretomes from HNECs using isobaric tag for relative and absolute quantification (iTRAQ). (*A*) A heat map showing the relative abundance of 3,506 proteins identified in the iTRAQ-ALI-4Ds dataset. The color key indicates the relative abundance of each protein (−3 to 3) across eight samples from the iTRAQ-ALI-4Ds dataset. (*B–D*) Volcano plots demonstrating fold changes in protein abundance between ALI 2D and ALI 6D (*B*), ALI 2D and ALI 10D (*C*), and ALI 2D and ALI 15D (*D*). The *x*-axis represents the log2 ratio, and the *y*-axis represents significant differences (−log10 of *P* value, $n = 2$). A total of 269 proteins were changed by at least twofold ($P < 0.01$, $n = 2$): ALI 2D versus ALI 6D (37 proteins), ALI 2D versus ALI 10D (112 proteins), and ALI 2D versus ALI 15D (120 proteins). (*E–G*) Temporal profiles of eight mucin family members. Tethered mucins MUC1, MUC4, and MUC16 (*E*); gel-forming mucins MUC5A and MUC5B (*F*); minor mucins MUC18, MUC20, and MUC21 (*G*). Numbers in parenthesis are the total numbers of identified peptide sequences (Σ# PSMs) for the protein. $^{**}P < 0.01$ by one-way ANOVA with Bonferroni *post hoc* correction.

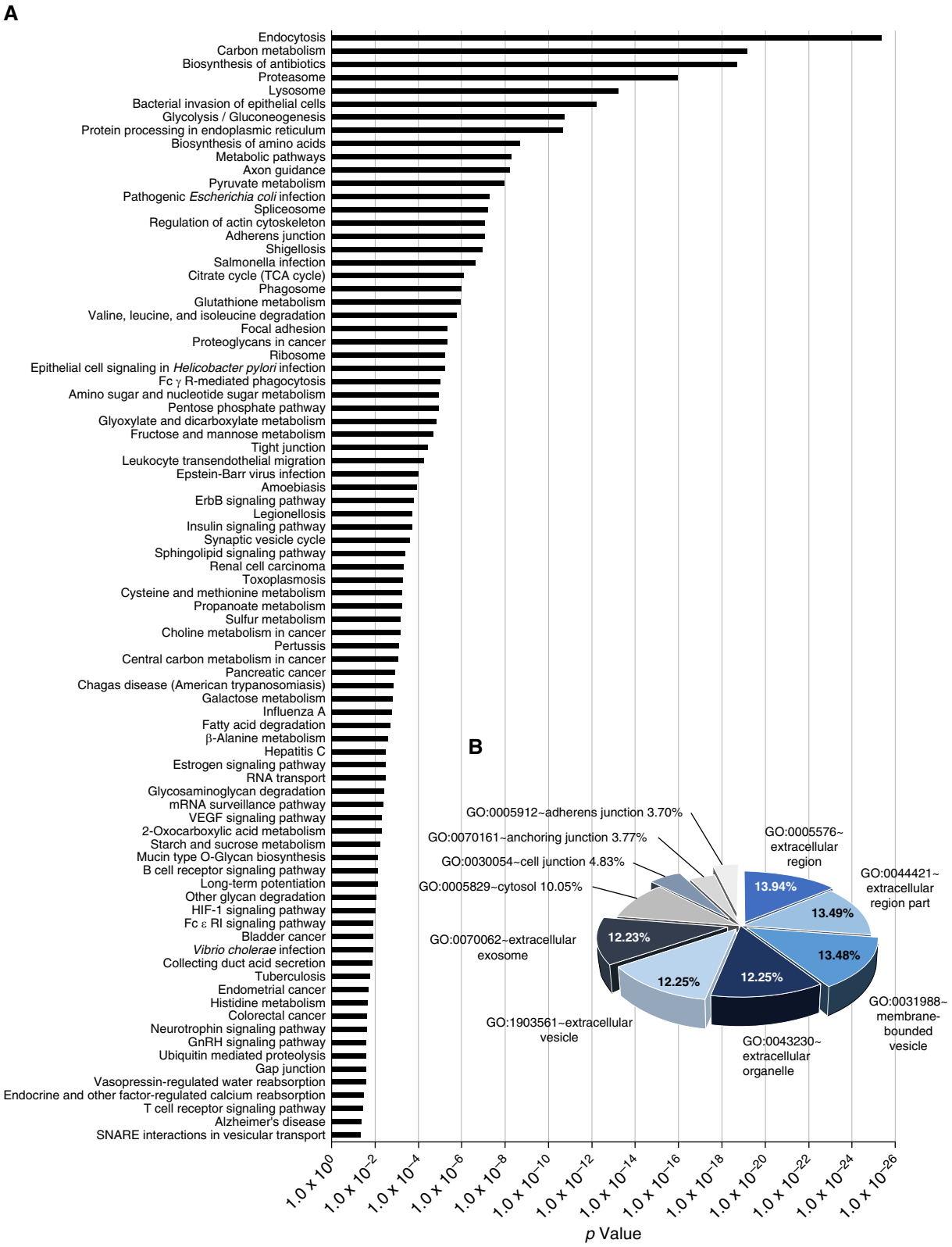

Figure 3. Characterization of proteins in HNEC secretomes. (*A*) Significant biological pathways enriched among 3,506 proteins identified by iTRAQ are represented as bar graphs. (*B*) Pie graph showing cellular localization of the HNEC secretomes classified by the top 10 cellular compartment in functional annotation with gene ontology analysis (GO). GnRH = gonadotropin-releasing hormone; HIF-1 = hypoxia-inducible factor 1; SNARE = SNAP receptor; TCA cycle = tricarboxylic acid cycle; VEGF = vascular endothelial growth factor. ErbB = erythroblastic leukemia viral oncogene homolog.

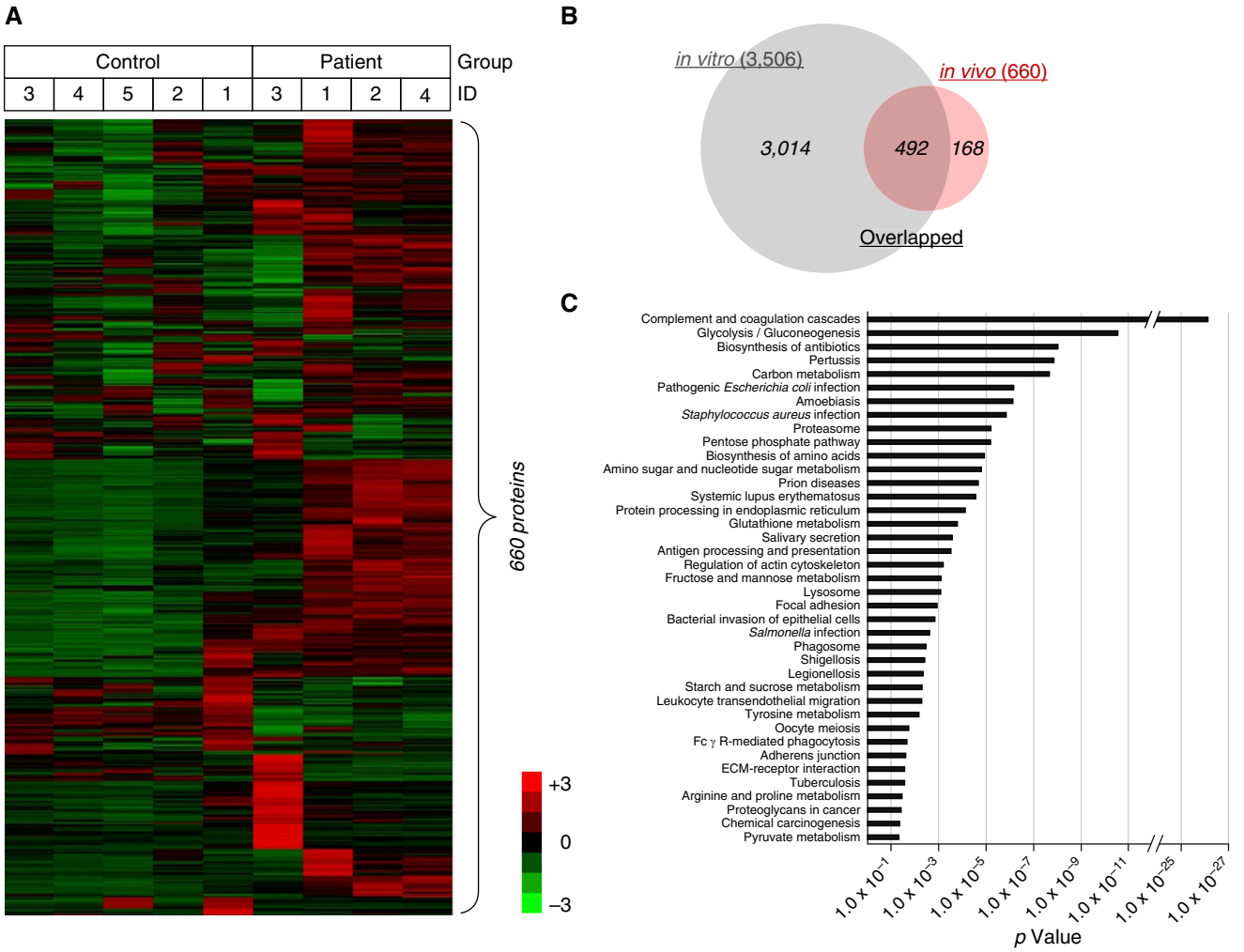

Figure 4. Characterization of secretomes from patients after endoscopic sinus surgery. (*A*) Heat map showing the relative abundance of 660 proteins identified in the iTRAQ-H9 dataset. The color key indicates the relative abundance of each protein (−3 to 3) across nine samples from the iTRAQ-H9 dataset. (*B*) Venn diagram showing overlapping proteins (492) between HNEC secretomes (*in vitro*) and patient secretomes (*in vivo*). (*C*) Significant biological pathways enriched among 660 secretome proteins are represented as bar graphs. ECM = extracellular matrix.

14.03% of 3,506 *in vitro* secretomes. Common inflammation biomarkers, which have been recently described (12–14), were secreted by more than twofold higher in patient NAL fluid secretomes than in control NAL fluid secretomes, such as eosinophil cationic protein ($P = 0.030$), serum albumin ($P = 0.004$), and myeloperoxidase ($P = 0.052$) (Table E7). Moreover, KEGG pathway analysis showed that 28 of the 39 enriched pathways in NAL fluid secretomes were shared with HNEC secretomes (71.80%; Figure 4C). Pathways enriched only in the NAL fluid secretomes were as follows: complement and coagulation cascades (35 proteins); systemic lupus erythematosus (20 proteins); *Staphylococcus aureus* infection (14 proteins); salivary secretion (14 proteins); antigen processing and presentation (13 proteins); oocyte meiosis (12 proteins); prion diseases (10 proteins); extracellular matrix–receptor interaction (10 proteins); chemical carcinogenesis (9 proteins); tyrosine metabolism (7 proteins); and arginine and proline metabolism (7 proteins). These pathways showed more physiological characteristics of *in vivo* biological specimens than *in vitro* cell culture samples (Figure 4C).

GO functional analysis revealed that the proportion of secreted proteins in the NAL fluid secretomes (74.59% of GO items in the top 10 CC categories) were larger than that in the HNEC secretomes (data not shown). After removing blood-derived proteins (e.g., immunoglobulin or fibrinogen chains), the top 50 abundant proteins in the NAL fluid secretomes were examined and listed by their Σ# PSMs in Table E3; 22 of them (44.00%) overlapped with the HNEC secretomes (Table E2). Most of the listed proteins of the NAL fluid secretomes were identified in previous proteomic analysis of human nasal secretion (20, 35). Although all subjects in this study had no allergic rhinitis, we detected highly secreted complement C3, alpha-1 antitrypsin, and APOA1, which are reported to be more abundant in patients with allergic rhinitis (20), suggesting that these secreted proteins could be elevated in both allergic and nonallergic inflammatory conditions.

Comparative Analysis of *In Vitro* Temporal Secretomes with *In Vivo* Human NAL Fluid Secretomes

Given that primary HNECs are the only culturable cells among the diverse cell types comprising the nasal mucosa, and that the regeneration of the cells in which basal cells were differentiated into mucociliary epithelium partially represents the regeneration process of the nasal mucosa after surgery (mechanical stress), we hypothesized that it could be possible to identify specific biomarkers of nasal mucosal inflammation by comparing *in vitro* HNEC secretomes with *in vivo* NAL fluid secretomes. To this goal, we rearranged the proteins of HNEC secretomes based on their temporal profiles. A total of 1,070 proteins was clustered into 4 classes corresponding to ALI days: cluster A contains 84 proteins secreted highly at ALI 2D; cluster B contains 246 proteins at ALI 6D; cluster C contains 664 proteins at ALI 10D; and cluster D contains 76 proteins at ALI 15D (Figure 5A; results of KEGG pathway analysis for each cluster are listed in Table E4). We also reanalyzed the iTRAQ-H9 raw dataset and found that 86 proteins were significantly changed by more than twofold in the patient group ($P < 0.05$, $n = 4$) compared with the control group ($n = 3$) (Figure 5B; results of KEGG pathway analysis for the 86 proteins from the NAL fluid secretomes are listed in Table E5). When biological pathways enriched in the NAL fluid secretome were compared with those enriched in each cluster of the HNEC secretome, we found that the NAL fluid secretome shared three pathways (50.00%) with cluster A (ALI 2D) of the HNEC secretome, two pathways (14.29%) with cluster B (ALI 6D), one pathway (3.33%) with cluster C (ALI 10D), and none with cluster D (ALI 15D). These results suggest that 2 weeks after surgery, the regeneration status of the patient's nasal mucosa is similar to that in the early stages of HNEC differentiation (ALI 2D and 6D; Tables E5 and E6).

To identify specific biomarkers of nasal mucosal inflammation, a parallel approach was used. In our first approach, we sought to select candidate proteins from the cluster-specific HNEC secretomes to compare with patient NAL fluid secretomes. Interestingly, we found that APOE, clusterin (also known as APOJ), and prolow-density lipoprotein receptor–related protein 1 (LRP1; also known as APOE receptor) were exclusively secreted at ALI 6D (Figure 5C). We also found that several APOs—APOA1, APOA2, APOB, APOC1, APOE, and APOM—showed significantly higher secretion in patient NAL fluid secretomes than in control NAL fluid secretomes (Figure 5D). Expression of APOE, which is the only overlapping protein, was validated by Western blotting in both HNEC secretions (Figure 5E) and human NAL fluids (Figure 5F). In our second approach, we selected 19 candidates by analyzing proteins that were increased in *in vivo* secretomes with publicly deposited microarray data using the GeneVisible tool (https://genevisible.com) (36): POSTN; GTP-binding protein RAD; aminopeptidase B; C4b-binding protein α chain; α-2-macroglobulin; chloride intracellular channel protein 6; nitric oxide synthase, inducible (NOS2); phosphomannomutase 2; thioredoxin domain–containing protein 17; serine/threonine-protein phosphatase 2A 65-kD regulatory subunit A α isoform; serum amyloid A-4 protein; sorcin; pregnancy zone protein; tubulin β chain; antithrombin-III; proteasome subunit β type-2; inter-α-trypsin inhibitor heavy chain H1; pancreatic secretory granule membrane major glycoprotein GP2; and retinoic acid receptor responder protein 1. By additional searching in the UniProt Databases for the physiological functions of these proteins (https://www.uniprot.org), we found that only two proteins, POSTN and NOS2, were possibly involved in inflammation. Given its contributions to mucus secretion, airway fibrosis, and remodeling (27), and its abundance (Σ# PSMs of POSTN [75 peptides] were much higher than those of NOS2 [8 peptides]), we selected POSTN as a candidate for further validation. Consistent with the iTRAQ analysis result showing highly secreted POSTN in patient NAL fluid secretomes (Figure 5D), Western blot analysis confirmed that the amount of secreted POSTN, the full length of which is 93 kD, increased dramatically in patient NAL fluid secretomes compared with that in control NAL fluid secretomes (Figure 5F). However, POSTN was not detected in HNEC secretomes (data not shown). These results are logical, because POSTN in patient NAL fluid secretomes could be induced by various inflammatory mediators secreted during mucosal wound regeneration after surgery, and could not be induced in HNEC secretomes under the culture conditions in which no inflammatory stimuli were present.

Characterization of APOE and POSTN Expressed in the Nasal Mucosa

To characterize the differential expression of APOE and POSTN, we performed immunohistochemical (IHC) analysis for the proteins on nasal mucosal sections from normal and pathological specimens. An IHC analysis of the nasal mucosa obtained from a patient with allergic rhinitis (AR) showed that strong immunoreactivity for APOE was detected in a portion of intermediate cell layers between basal cells and fully differentiated cells (Figure 6A, middle panel), whereas POSTN immunoreactive signal was exclusively presented in the subepithelial connective tissue (Figure 6B, middle panel), which was consistent with previous studies (26, 28, 37), suggesting that most of the identified POSTN in the *in vivo* secretomes may originate from the subepithelial connective tissue of patients with CRS whose injured nasal mucosa were in regeneration.

Discussion

Most previous proteomics studies have analyzed secreted proteins either *in vitro* only (6, 7, 17, 18, 38) or *in vivo* only (19, 20, 35, 39–42). We found only one study in which the authors compared the composition of apical secretions from human tracheobronchial epithelial cells (HTBECs) and sputum induced from the airways of normal individuals (43). In our study, we compared two distinct proteomics data sets, *in vitro* secretomes and *in vivo* secretomes, to identify candidate biomarkers of nasal mucosal inflammation. Using a parallel approach, we identified APOE as a differentiation stage–specific biomarker in the apical secretions of HNECs and POSTN as an epithelium-derived inducible biomarker in patients' NAL fluids. In the first approach to select candidates for nasal epithelial cell–derived biomarkers, we screened the increased proteins from *in vitro* secretomes in primary HNEC cultures according to the degree of differentiation, and then selected the overlapping proteins that were

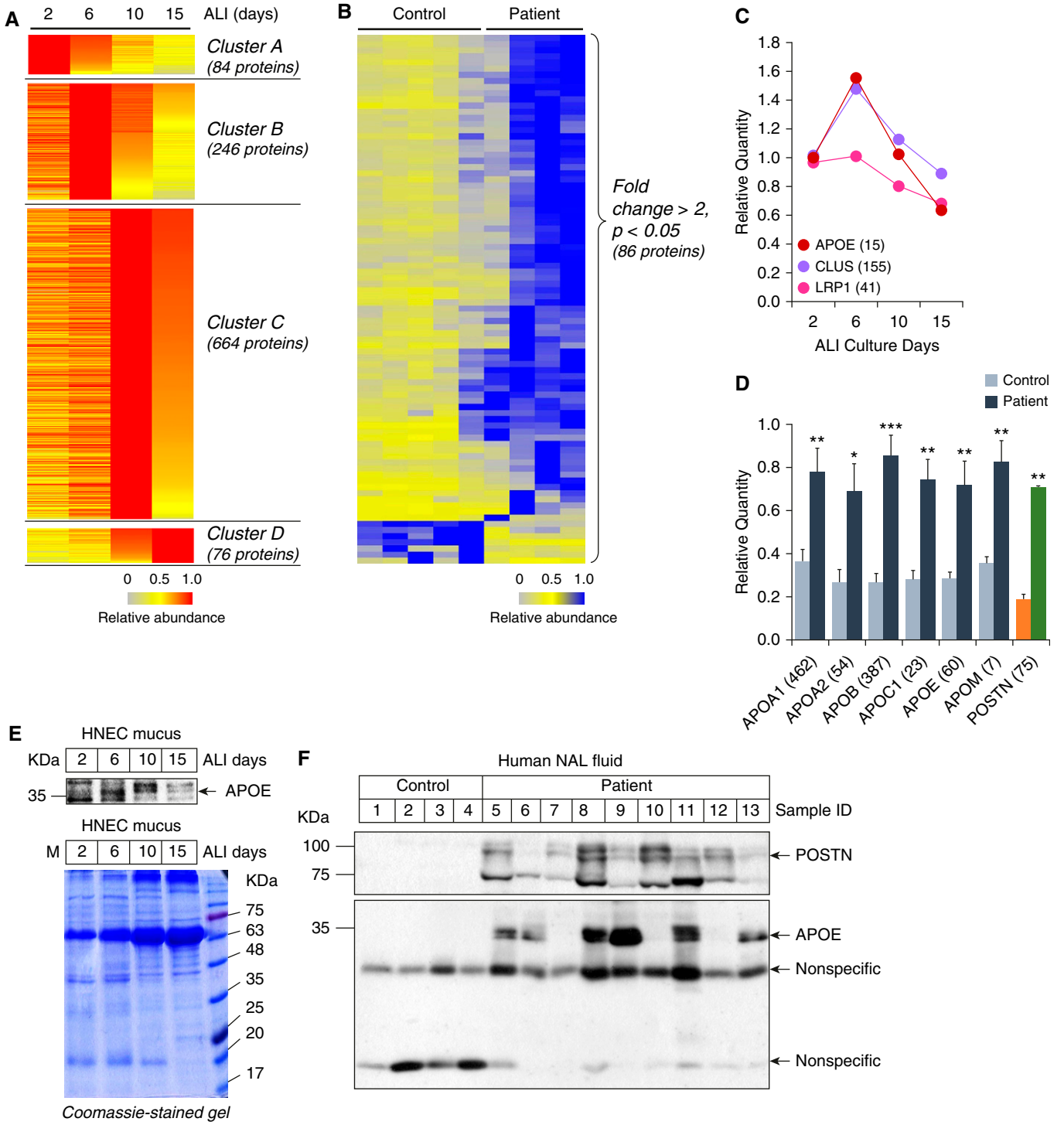

Figure 5. Comparison between *in vitro* and *in vivo* secretomes. (*A*) Heat map showing four clusters of *in vitro* secretome proteins based on their temporal profiles: cluster A (84 proteins secreted highly at ALI 2D); cluster B (246 proteins at ALI 6D); cluster C (664 proteins at ALI 10D); and cluster D (76 proteins at ALI 15D). (*B*) Heat map showing 86 *in vivo* secretome proteins with high abundance in patient group (FC > 2, $P < 0.05$). (*C*) Temporal profiles of three apolipoproteins (APOs): APOE; clusterin (CLUS; also known as APOJ); and prolow-density lipoprotein receptor–related protein 1 (LRP1, also known as ApoE receptor). (*D*) Relative quantities of APOs and periostin (POSTN) in *in vivo* secretome samples from nasal lavage (NAL) fluid of patients and that of control subjects are presented as bar graphs. Numbers in parenthesis are the Σ# PSMs for the protein. Results are the means ± SEM; $^{*}P < 0.05$, $^{**}P < 0.01$, and $^{***}P < 0.001$ versus control group. (*E*) Amount of ApoE in *in vitro* secretome samples isolated from HNECs cultures during differentiation were analyzed by Western blotting (upper panel). Gels were stained with Coomassie blue (lower panel). (*F*) Amount of POSTN and ApoE in NAL fluid secretomes was analyzed by Western blotting (upper panel). Gels were stained with Coomassie blue (lower panel). FC = fold change.

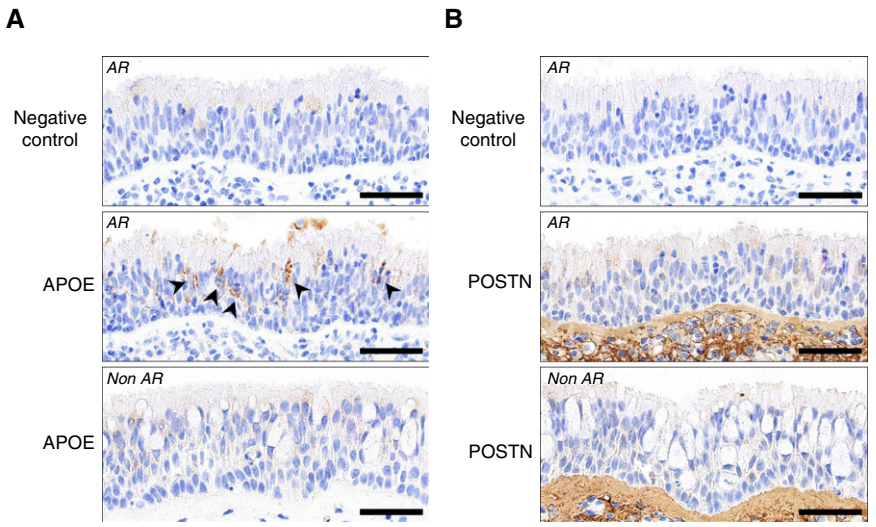

Figure 6. Expression of APOE and POSTN in the nasal mucosa. Nasal mucosal sections from a patient with allergic rhinitis (AR) stained with antibodies against APOE (*A*, middle panel) or POSTN (*B*, middle panel), or without primary antibodies (negative control, top panels of *A* and *B*). Arrowheads indicate the APOE immunoreactive signals. Nasal mucosal sections from a patient without AR (Non AR, bottom panels) stained with antibodies against APOE (*A*, bottom panel) or POSTN (*B*, bottom panel) as control. Scale bars: 50 μm.

increased in *in vivo* secretomes from the patients. A disadvantage of this approach is that inflammatory mediator–inducible proteins could not be detected during the differentiation process throughout the culture. To compensate for this disadvantage, as the second approach, we screened the increased proteins in *in vivo* secretomes from the patients, and then selected the proteins known to be expressed in the human nasal epithelium.

To screen the increased proteins from *in vitro* secretomes according to the degree of differentiation, we established a temporal proteomic approach using multiplexed iTRAQ, in which a maximum eight individual secretion samples can be quantitatively examined simultaneously. Moreover, in contrast to previous studies in which secretions were harvested at a single point of ALI culture, airway surface liquid from HNECs at ALI 14D (17, 38), apical and basolateral secretions from human bronchial epithelial cells (HBECs) at ALI 21D (17), apical surface fluid HTBECs at ALI 28D (18, 43), or apical secretions from HTBECs at ALI 42D (43), we collected secretions from HNECs at different time points from ALI D2 to ALI D15 (Figure 2A). By analyzing these secretomes using multiplexed iTRAQ, our temporal proteomic approach is advantageous for investigating not only the presence of interesting proteins, but also their dynamic changes in apical secretions during HNEC differentiation. It usually takes 3–4 months for complete mucosal regeneration after endoscopic sinus surgery. We have collected NAL fluid from patients at 2 weeks after sinus surgery, as it is the most clinically active period of mucosal regeneration. It would be more intriguing to obtain patient samples at different time points during the recovery of sinus surgery and to compare their *in vivo* longitudinal proteomes with the *in vitro* secretomes that are dramatically changing upon cell differentiation.

Although many *in vivo* proteomics studies have investigated secretions from the upper airway (e.g., nasal mucus [19, 20, 39–41] and NAL fluid [35, 42]), no *in vitro* studies have used upper airway–derived cells; lower airway–derived cells used in *in vitro* studies include HBECs (6, 17, 38), HTBECs (18, 43), and human airway gland in tracheal tissues (7). Thus, this is the first study to analyze secretomes originating from HNECs by quantitative proteomics. Using our established primary culture system of HNECs (44), we recently reported that the innate immune system response to house dust mites differed between the nose and the lung (45). However, large portions of the secretomes in this study overlapped with secretomes in previous studies, indicating that the upper and lower airway secretions have similar secreted protein profiles, although the two tissues have embryologically different origins—the nose originates from the ectoderm and the lung from the mesoderm and endoderm—and they differ in their microenvironments in terms of the microbiome present (46).

Given the critical function of the mucus layer in protecting the airway surface against pathogens in the host defense mechanism (47–49), our iTRAQ data were compared with proteome lists of protective proteins with "anti"-activities, including antimicrobial, antiinflammatory, antiproteolytic, and antiantioxidant activities (6, 7). We found 19 protective proteins in HNEC secretomes with anti-activities: serotransferin, α-1-antichymotrypsin, lumican, and 40S ribosomal protein SA were highly secreted at ALI 2D (Figure 5A, cluster A); neutrophil gelatinase-associated lipocalin and β-2-microglobulin were secreted at ALI 6D (Figure 5A, cluster B); glutathione *S*-transferase P, thioredoxin, superoxide dismutase [Mn], mitochondrial, and S10A6 were secreted at ALI 10D (Figure 5A, cluster C); and annexin A2, CERU, aldehyde dehydrogenase, bacterial/permeability-increasing fold-containing family B member 1, histone H4, serpin B3, and polymeric immunoglobulin receptor were secreted highly at ALI 15D (Figure 5A, cluster D). Two exosome-related proteins, myosin light polypeptide 6 and erythrocyte band 7 integral membrane protein, the peptides of which were detected in apical secretions from HBECs (17), were also detected in our HNEC secretomes; however, the expression profiles were not significantly altered during differentiation (data not shown). The iTRAQ technique we used here has two remarkable advantages for studying mucus secretions: its gel-free and multiplex labeling characteristics that enhance sensitivity and resolution, and the ability to monitor dynamic changes of proteins.

Gel-free proteomic approaches have several advantages compared with gel-based proteomics, particularly for identifying membrane-bound and/or glycosylated large proteins (e.g., mucins) (50). Notably, large amounts of transmembrane mucins, MUC16 (785 peptides) and MUC1 (574 peptides), were detected in the HNEC secretomes using our gel-free iTRAQ proteomic method (Table E2), whereas the

secreted amount was very low (16 peptides) in the NAL fluid secretomes, indicating that MUC16 is secreted mainly by epithelial cells and not induced under pathophysiological conditions (e.g., nasal mucosa regeneration). Although MUC16 contributes to epithelial barrier function and immune homeostasis in corneal epithelial cells (51, 52), further studies of the biological functions of MUC16 in the nasal epithelium are needed.

Many other proteins in the list of the top 50 most abundant proteins in the HNEC secretomes (Table E2) were also detected at higher levels than in previous gel-based proteomics studies (6, 17, 18); α-1-antichymotrypsin, annexin A1, annexin A2, cathepsin D, CERU, complement C3, α-enolase, ezrin, galectin-3–binding protein, gelsolin, glutathione *S*-transferase P, neutrophil gelatinase–associated lipocalin, polymeric immunoglobulin receptor, and protein S100-A8 were also found in a study using HBECs (6); sodium-dependent phosphate, α-actinin-1, actin, cytoplasmic 1, and serpin B4, transport protein 2B, serum albumin, complement factor B, and α-actinin-4 were also found in the apical compartment of HBECs (17). Protein S100-A9 and heat shock cognate 71-kD protein were also found in a study using HTBECs (18). In many cases, Σ# PSMs were 10- to 100-fold higher in our study than in other gel-based proteomics studies, indicating that gel-free proteomic methods can identify more proteins. However, most of the identified proteins in this study were not suggested as biomarkers, as their secretions in patients' NAL fluids were not significantly changed.

APOE was secreted specifically at ALI 6D of HNEC differentiation and secreted at higher levels in patient NAL fluid secretomes (2.50-fold, $P = 0.0038$). APOA1, APOA2, or APOH were previously detected by nasal mucus proteomics analysis (19, 20, 35, 39, 42), whereas APOE was not previously detected. This is the first report to detect increased APOE together with its receptor, LRP1, in primary human airway epithelial cells. The Σ# PSMs for these proteins support that the proteins originated from the nasal epithelium and not from other types of cells (15 peptides for APOE and 41 peptides for LRP1). APOE, a 34-kD APO, is primarily synthesized by hepatocytes, and plays a critical role in lipid homeostasis, but its biological effects are not limited to vascular biology, because APOE is also expressed by type I and II alveolar epithelial cells, retinal pigment epithelial cells, pulmonary artery smooth muscle cells, alveolar macrophages, as well as in the central nervous system (53, 54). Our IHC data clearly show that APOE was expressed by the nasal epithelial cells. However, further in-depth investigations will be required to fully define the expression of APOE in a distinct subpopulation of the nasal epithelial cells.

Although the transcriptome-based database revealed that the top 10 POSTN-enriched tissues did not include the epithelium (data not shown), a recent study reported that POSTN is induced in airway epithelium in response to IL-13 stimulation (55, 56). Fahy and coworkers found that POSTN is secreted from primary HBECs by IL-13 treatment, and is specifically increased in the bronchial epithelium of patients with asthma (55). Thus, these results suggest that nasal epithelial cell–derived POSTN is a good candidate for human nasal mucosal inflammation. Although POSTN appears to be nonspecifically expressed at high levels in patients affected by conditions associated with increased cell division, cell turnover, cell invasion, and angiogenesis, its role in asthma, allergic rhinitis, and CRS with nasal polyp has been intensively investigated (37, 57). Consistent with our results, POSTN is a potent biomarker of mucosal remodeling in CRS because of its association with basement membrane thickening, fibrosis, and tissue eosinophilia (58). Here, we have identified and suggested APOE and POSTN as possible biomarkers of nasal mucosal inflammation. These findings provide new insights into how nasal epithelium–derived proteins are determined to be biomarkers of nasal inflammatory diseases. ■

Author disclosures are available with the text of this article at www.atsjournals.org.

References

1. Rogers DF. Airway goblet cells: responsive and adaptable front-line defenders. *Eur Respir J* 1994;7:1690–1706.
2. Mercer RR, Russell ML, Roggli VL, Crapo JD. Cell number and distribution in human and rat airways. *Am J Respir Cell Mol Biol* 1994;10:613–624.
3. Boers JE, Ambergen AW, Thunnissen FB. Number and proliferation of basal and parabasal cells in normal human airway epithelium. *Am J Respir Crit Care Med* 1998;157:2000–2006.
4. Rock JR, Onaitis MW, Rawlins EL, Lu Y, Clark CP, Xue Y, *et al*. Basal cells as stem cells of the mouse trachea and human airway epithelium. *Proc Natl Acad Sci USA* 2009;106:12771–12775.
5. Rock JR, Randell SH, Hogan BL. Airway basal stem cells: a perspective on their roles in epithelial homeostasis and remodeling. *Dis Model Mech* 2010;3:545–556.
6. Ali M, Lillehoj EP, Park Y, Kyo Y, Kim KC. Analysis of the proteome of human airway epithelial secretions. *Proteome Sci* 2011;9:4.
7. Joo NS, Evans IA, Cho HJ, Park IH, Engelhardt JF, Wine JJ. Proteomic analysis of pure human airway gland mucus reveals a large component of protective proteins. *PLoS One* 2015;10:e0116756.
8. Broide DH, Finkelman F, Bochner BS, Rothenberg ME. Advances in mechanisms of asthma, allergy, and immunology in 2010. *J Allergy Clin Immunol* 2011;127:689–695.
9. Davies DE. The role of the epithelium in airway remodeling in asthma. *Proc Am Thorac Soc* 2009;6:678–682.
10. Lü FX, Esch RE. Novel nasal secretion collection method for the analysis of allergen specific antibodies and inflammatory biomarkers. *J Immunol Methods* 2010;356:6–17.
11. Riechelmann H, Deutschle T, Friemel E, Gross HJ, Bachem M. Biological markers in nasal secretions. *Eur Respir J* 2003;21: 600–605.
12. Wang JH, Devalia JL, Duddle JM, Hamilton SA, Davies RJ. Effect of six-hour exposure to nitrogen dioxide on early-phase nasal response to allergen challenge in patients with a history of seasonal allergic rhinitis. *J Allergy Clin Immunol* 1995;96: 669–676.
13. Wålinder R, Norbäck D, Wieslander G, Smedje G, Erwall C, Venge P. Nasal patency and biomarkers in nasal lavage—the significance of air exchange rate and type of ventilation in schools. *Int Arch Occup Environ Health* 1998;71:479–486.
14. Norbäck D, Wålinder R, Wieslander G, Smedje G, Erwall C, Venge P. Indoor air pollutants in schools: nasal patency and biomarkers in nasal lavage. *Allergy* 2000;55:163–170.
15. Riechelmann H, Deutschle T, Rozsasi A, Keck T, Polzehl D, Bürner H. Nasal biomarker profiles in acute and chronic rhinosinusitis. *Clin Exp Allergy* 2005;35:1186–1191.
16. Tomassen P, Vandeplas G, Van Zele T, Cardell LO, Arebro J, Olze H, *et al*. Inflammatory endotypes of chronic rhinosinusitis based on cluster analysis of biomarkers. *J Allergy Clin Immunol* 2016;137: 1449–1456.e4.

17. Pillai DK, Sankoorikal BJ, Johnson E, Seneviratne AN, Zurko J, Brown KJ, *et al*. Directional secretomes reflect polarity-specific functions in an in vitro model of human bronchial epithelium. *Am J Respir Cell Mol Biol* 2014;50:292–300.
18. Kim SW, Cheon K, Kim CH, Yoon JH, Hawke DH, Kobayashi R, *et al*. Proteomics-based identification of proteins secreted in apical surface fluid of squamous metaplastic human tracheobronchial epithelial cells cultured by three-dimensional organotypic air–liquid interface method. *Cancer Res* 2007;67:6565–6573.
19. Tomazic PV, Birner-Gruenberger R, Leitner A, Darnhofer B, Spoerk S, Lang-Loidolt D. Apolipoproteins have a potential role in nasal mucus of allergic rhinitis patients: a proteomic study. *Laryngoscope* 2015; 125:E91–E96.
20. Tomazic PV, Birner-Gruenberger R, Leitner A, Obrist B, Spoerk S, Lang-Loidolt D. Nasal mucus proteomic changes reflect altered immune responses and epithelial permeability in patients with allergic rhinitis. *J Allergy Clin Immunol* 2014;133: 741–750.
21. Singh K, Chaturvedi R, Asim M, Barry DP, Lewis ND, Vitek MP, *et al*. The apolipoprotein E-mimetic peptide COG112 inhibits the inflammatory response to Citrobacter rodentium in colonic epithelial cells by preventing NF-κB activation. *J Biol Chem* 2008;283: 16752–16761.
22. Yao X, Remaley AT, Levine SJ. New kids on the block: the emerging role of apolipoproteins in the pathogenesis and treatment of asthma. *Chest* 2011;140:1048–1054.
23. El-Bahrawy AH, Tarhuni A, Kim H, Subramaniam V, Benslimane I, Elmageed ZYA, *et al*. Correction: ApoE deficiency promotes colon inflammation and enhances the inflammatory potential of oxidized-LDL and TNF-α in primary colon epithelial cells. *Biosci Rep* 2016;36: pii:e00408.
24. Vuilleumier N, Dayer JM, von Eckardstein A, Roux-Lombard P. Pro- or anti-inflammatory role of apolipoprotein A-1 in high-density lipoproteins? *Swiss Med Wkly* 2013;143:w13781.
25. Eline Slagboom P, van den Berg N, Deelen J. Phenome and genome based studies into human ageing and longevity: an overview. *Biochim Biophys Acta Mol Basis Dis* 2018;1864:2742–2751.
26. Masuoka M, Shiraishi H, Ohta S, Suzuki S, Arima K, Aoki S, *et al*. Periostin promotes chronic allergic inflammation in response to Th2 cytokines. *J Clin Invest* 2012;122:2590–2600.
27. O'Dwyer DN, Moore BB. The role of periostin in lung fibrosis and airway remodeling. *Cell Mol Life Sci* 2017;74:4305–4314.
28. Izuhara K, Nunomura S, Nanri Y, Ogawa M, Ono J, Mitamura Y, *et al*. Periostin in inflammation and allergy. *Cell Mol Life Sci* 2017;74: 4293–4303.
29. Xu M, Chen D, Zhou H, Zhang W, Xu J, Chen L. The role of periostin in the occurrence and progression of eosinophilic chronic sinusitis with nasal polyps. *Sci Rep* 2017;7:9479.
30. Chung YW, Lagranha C, Chen Y, Sun J, Tong G, Hockman SC, *et al*. Targeted disruption of PDE3B, but not PDE3A, protects murine heart from ischemia/reperfusion injury. *Proc Natl Acad Sci USA* 2015;112: E2253–E2262.
31. Wang BY, Gil J, Kaufman D, Gan L, Kohtz DS, Burstein DE. P63 in pulmonary epithelium, pulmonary squamous neoplasms, and other pulmonary tumors. *Hum Pathol* 2002;33:921–926.
32. Rose MC, Voynow JA. Respiratory tract mucin genes and mucin glycoproteins in health and disease. *Physiol Rev* 2006;86:245–278.
33. Thai P, Loukoianov A, Wachi S, Wu R. Regulation of airway mucin gene expression. *Annu Rev Physiol* 2008;70:405–429.
34. Thornton DJ, Rousseau K, McGuckin MA. Structure and function of the polymeric mucins in airways mucus. *Annu Rev Physiol* 2008;70: 459–486.
35. Wang H, Gottfries J, Barrenäs F, Benson M. Identification of novel biomarkers in seasonal allergic rhinitis by combining proteomic, multivariate and pathway analysis. *PLoS One* 2011;6:e23563.
36. Hruz T, Laule O, Szabo G, Wessendorp F, Bleuler S, Oertle L, *et al*. Genevestigator v3: a reference expression database for the meta-analysis of transcriptomes. *Adv Bioinforma* 2008;2008:420747.
37. Ishida A, Ohta N, Suzuki Y, Kakehata S, Okubo K, Ikeda H, *et al*. Expression of pendrin and periostin in allergic rhinitis and chronic rhinosinusitis. *Allergol Int* 2012;61:589–595.
38. Candiano G, Bruschi M, Pedemonte N, Musante L, Ravazzolo R, Liberatori S, *et al*. Proteomic analysis of the airway surface liquid: modulation by proinflammatory cytokines. *Am J Physiol Lung Cell Mol Physiol* 2007;292:L185–L198.
39. Tomazic PV, Birner-Gruenberger R, Leitner A, Spoerk S, Lang-Loidolt D. Seasonal proteome changes of nasal mucus reflect perennial inflammatory response and reduced defence mechanisms and plasticity in allergic rhinitis. *J Proteomics* 2016;133:153–160.
40. Al Badaai Y, DiFalco MR, Tewfik MA, Samaha M. Quantitative proteomics of nasal mucus in chronic sinusitis with nasal polyposis. *J Otolaryngol Head Neck Surg* 2009;38:381–389.
41. Tewfik MA, Latterich M, DiFalco MR, Samaha M. Proteomics of nasal mucus in chronic rhinosinusitis. *Am J Rhinol* 2007;21:680–685.
42. Casado B, Pannell LK, Iadarola P, Baraniuk JN. Identification of human nasal mucous proteins using proteomics. *Proteomics* 2005;5: 2949–2959.
43. Kesimer M, Kirkham S, Pickles RJ, Henderson AG, Alexis NE, Demaria G, *et al*. Tracheobronchial air–liquid interface cell culture: a model for innate mucosal defense of the upper airways? *Am J Physiol Lung Cell Mol Physiol* 2009;296:L92–L100.
44. Yoon JH, Kim KS, Kim SS, Lee JG, Park IY. Secretory differentiation of serially passaged normal human nasal epithelial cells by retinoic acid: expression of mucin and lysozyme. *Ann Otol Rhinol Laryngol* 2000;109:594–601.
45. Ryu JH, Yoo JY, Kim MJ, Hwang SG, Ahn KC, Ryu JC, *et al*. Distinct TLR-mediated pathways regulate house dust mite-induced allergic disease in the upper and lower airways. *J Allergy Clin Immunol* 2013; 131:549–561.
46. Huffnagle GB, Dickson RP, Lukacs NW. The respiratory tract microbiome and lung inflammation: a two-way street. *Mucosal Immunol* 2017;10:299–306.
47. Knowles MR, Boucher RC. Mucus clearance as a primary innate defense mechanism for mammalian airways. *J Clin Invest* 2002;109: 571–577.
48. Wine JJ, Joo NS. Submucosal glands and airway defense. *Proc Am Thorac Soc* 2004;1:47–53.
49. Bals R, Hiemstra PS. Innate immunity in the lung: how epithelial cells fight against respiratory pathogens. *Eur Respir J* 2004;23:327–333.
50. Rabilloud T. Membrane proteins and proteomics: love is possible, but so difficult. *Electrophoresis* 2009;30:S174–S180.
51. Gipson IK, Spurr-Michaud S, Tisdale A, Menon BB. Comparison of the transmembrane mucins MUC1 and MUC16 in epithelial barrier function. *PLoS One* 2014;9:e100393.
52. Menon BB, Kaiser-Marko C, Spurr-Michaud S, Tisdale AS, Gipson IK. Suppression of Toll-like receptor–mediated innate immune responses at the ocular surface by the membrane-associated mucins MUC1 and MUC16. *Mucosal Immunol* 2015;8:1000–1008.
53. Yao X, Gordon EM, Figueroa DM, Barochia AV, Levine SJ. Emerging roles of apolipoprotein E and apolipoprotein A-I in the pathogenesis and treatment of lung disease. *Am J Respir Cell Mol Biol* 2016;55: 159–169.
54. Gordon EM, Yao X, Xu H, Karkowsky W, Kaler M, Kalchiem-Dekel O, *et al*. Apolipoprotein E is a concentration-dependent pulmonary danger signal that activates the NLRP3 inflammasome and IL-1β secretion by bronchoalveolar fluid macrophages from asthmatic subjects. *J Allergy Clin Immunol* [online ahead of print] 11 Mar 2019; DOI: 10.1016/j.jaci.2019.02.027.
55. Sidhu SS, Yuan S, Innes AL, Kerr S, Woodruff PG, Hou L, *et al*. Roles of epithelial cell–derived periostin in TGF-beta activation, collagen production, and collagen gel elasticity in asthma. *Proc Natl Acad Sci USA* 2010;107:14170–14175.
56. Ito Y, Al Mubarak R, Roberts N, Correll K, Janssen W, Finigan J, *et al*. IL-13 induces periostin and eotaxin expression in human primary alveolar epithelial cells: comparison with paired airway epithelial cells. *PLoS One* 2018;13:e0196256.
57. Nair P, Kraft M. Serum periostin as a marker of T(H)2-dependent eosinophilic airway inflammation. *J Allergy Clin Immunol* 2012;130: 655–656.
58. Ebenezer JA, Christensen JM, Oliver BG, Oliver RA, Tjin G, Ho J, *et al*. Periostin as a marker of mucosal remodelling in chronic rhinosinusitis. *Rhinology* 2017;55:234–241.